Journal of Geodynamics 128 (2019) 1–10

Contents lists available at ScienceDirect

Journal of Geodynamics

journal homepage: www.elsevier.com/locate/jog

Sea level changes and vertical land motion from altimetry and tide gauges in the Southern Levantine Basin

Bayoumy Mohamed[a,*], Abdallah Mohamed[a], Khaled Alam El-Din[a], Hazem Nagy[a], Ahmed Elsherbiny[b]

[a] University of Alexandria, Faculty of Science, Department of Oceanography, Alexandria, Egypt
[b] Coastal Research Institute, 15 El Pharaana Street, El Shallalat, Alexandria, 21514, Egypt

ARTICLE INFO

Keywords:
Vertical land motion
Sea level change
Relative sea level
Satellite altimetry
Nile Delta

ABSTRACT

We have investigated the sea level rise (SLR) in the Southern Levantine region of the Mediterranean Sea during the period 1993–2015 using satellite altimetry and tide gauge data. Satellite altimetry indicated a positive SLR with a mean of 3.51 ± 0.62 mm/year, which is slightly higher than the global averaged mean SLR that was reported about 3.19 ± 0.63 (Chambers et al., 2017). The rates of vertical land motion (VLM rate) have been estimated from the trend of de-seasoned sea level difference (altimetry minus TG) time series at the 6 selected TG sites. Land subsidence was found to occur at three stations along the Nile Delta coast (Rosetta, Burullus and Damietta) and at one station in Israel (Hadera). Most of the previous studies in the Mediterranean Sea indicated that there are no sufficient tide gauge data in the Southern and Eastern Mediterranean Sea. So, this investigation offers valuable sea level information that can be applied in a wide range of climatology, related environmental issues, for example; land subsidence, inundation, and global warming in the southern Levantine basin.

1. Introduction

The southern Levantine sub-basin extends from 30 °N to 33.25 °N and from 25 °E to 34.5 °E. The longest coast along the southern Levantine region is that of Egypt (Fig. 1). The maximum depth of the studied area is about 3000 m in front of Mersa-Matruh city, in the western side of the Egyptian coast (Nagy et al., 2017). The Mediterranean cost of Egypt, especially that along the Nile Delta have been classified as one of the most five regions expected to experience the worst effects of the SLR of 1 m (Dasgupta et al., 2009). The global SLR in response to climate change has important implications, such as coastal erosion of beaches, inundation of low-lying coastal regions, increasing risk of flooding during storm surges, increasing salinization of coastal aquifers, and loss of the coastal ecosystem (Nicholls and Cazenave, 2010). Solomon et al. (2007) showed that the SLR is not uniform for the whole globe. Strong dependence on the local factors (e.g. subsidence/uplift due to compaction of the ground, pumping up of ground water, or neotectonism) creates a demand for better estimates of regional sea level variations as well as a better understanding of the physical factors causing them. So, assessments of regional and local SLR are essential for policy and decision makers responding to, and preparing for the impacts of sea level changes.

Tide gauges measure sea level change relative to a benchmark located on land. Thus, their measurements include land movements affecting the benchmark, while satellite altimeters measure sea level change with respect to the center of mass of the Earth. During the last two decades, a lot of previous studies used a combination of altimetry and TG data, to estimate the vertical land motion in the Mediterranean Sea (Fenoglio-Marc et al., 2004; García et al., 2011; Wöppelmann and Marcos, 2012). However, most of these studies suffered from lack of tide gauges data in the southern Levantine region especially along the Egyptian Mediterranean coast. Recent studies demonstrate an increase in Mediterranean mean sea level of 3 mm/year (Tsimplis et al., 2013) from altimetric data during1993–2011. Bonaduce et al. (2016) supported Haddad et al. (2013), finding that during the 1993–2012 period, the mean sea level displayed a significant positive trend of 2.44 mm/year. Shaltout et al. (2015) showed that the absolute dynamic topography from satellite altimetry are highly correlated with tide gauge observations along the Egyptian Mediterranean coast. Consequently, the satellite altimetry sea level data can be used to study coastal sea level changes in the study area. They found that the average rate of SLR in the southern Levantine sub-basin is 3.1 mm/year during the period (1993–2013), and the averaged of the absolute dynamic topography during the study period was ranged from -17 cm to 8 cm. The sea level

* Corresponding author.
E-mail address: bayomi.mabrouk@alexu.edu.eg (B. Mohamed).

https://doi.org/10.1016/j.jog.2019.05.007
Received 13 December 2017; Received in revised form 2 May 2018; Accepted 19 May 2019
Available online 20 May 2019

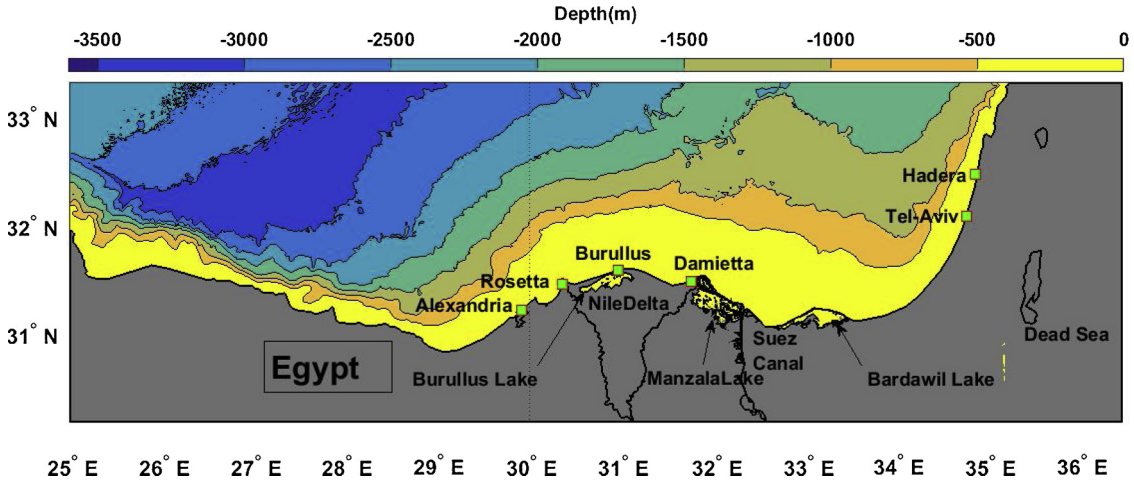

Fig. 1. Bathymetric chart and the location of the tide gauges used in this study (squares).

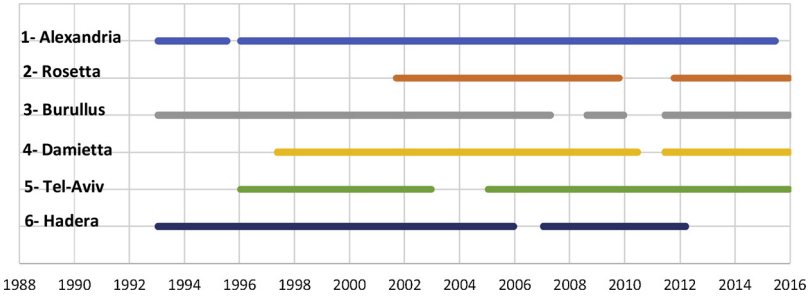

Fig. 2. Time availability of the tide gauge data at different stations (numbered according to Table1).

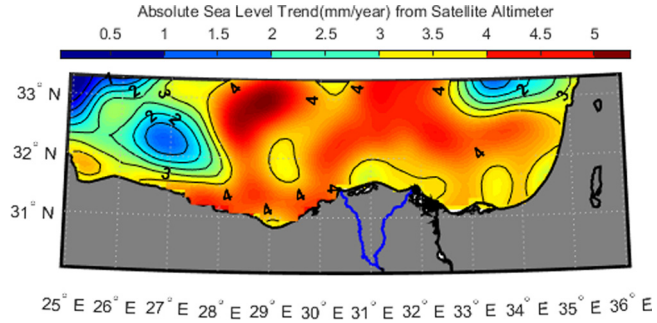

Fig. 3. Map of the Southern Levantine Basin sea level trends derived from merged satellite altimetry during the period 1993–2015.

variation is significantly affected by steric effect, and sea level variation west of the Gibraltar Strait.

Recent studies on sea level changes and land subsidence in the southern Levantine sub-basin have indicated that; the Nile Delta coast is subjected to relatively high rates of subsidence of - 4 to -5 mm/year (Ericson et al., 2006; El-Din et al., 2007; Stanley and Toscano, 2009). Raey (2010) estimated that even with a resulted SLR of only 0.5 m, roughly all the Nile Delta beaches and approximately 30% of the cities of Port Said and Alexandria will be eroded and damaged. Frihy et al. (2010) showed that, a continuous rise in mean sea level fluctuating between 1.8 and 4.9 mm/year, are obtained from 5 TG stations (Alexandria, Rosetta, Burullus, Damietta, and Port Said), the higher rate occurs at the Rosetta promontory, while the smaller one was at the Alexandria harbor. Also, land subsidence rate has been estimated; the maximum value was observed at Rosetta (- 4 mm/year), while the minimum one was observed at Alexandria (0 mm/year). Wöppelmann et al. (2013) showed that most of the coastline of Alexandria has been subjected to moderate land subsidence over the past decade (with average of −0.4 mm/year and up to −2 mm/year locally).

After the building of Aswan High Dam, the Nile Delta coasts became more vulnerable to inundation due to land subsidence only, even in the absence of any rise in sea level (Hassaan and Abdrabo, 2013). A more serious issue of sediment trapped by the dam is that it has increased coastline erosion surrounding the Nile Delta. The Nile Delta aquifer in Egypt is being additionally subjected to a severe seawater intrusion problem. Bonaduce et al. (2016) showed that the SLR in Israel at Hadera station, was about 5 ± 0.1 mm/year from tide gauge and about 2.29 ± 0.09 mm/year from altimetry data during 1993–2012. Stanley and Clemente (2017) indicated that subsidence in Egypt's Nile delta are due to three factors neotectonic lowering, compaction of Holocene sequences, and decreased sediment replenishment by much reduced Nile stream to Egypt's coast. Land subsidence rates accounts for variable average of about −3.7 mm/year of section in the north-west delta, −7.7 mm/year in the north delta, and -8.4 mm/year in the north-east delta, based on compaction rates of strata thicknesses that declined down-core between top and base of Holocene sections in 85 drill cores distributed along the Nile Delta margin.

This article aims to: (1) provide a comprehensive and up-to-date assessment of sea level changes in the Southern Levantine region using altimetry and tide gauge data. (2) estimate the vertical land motion (VLM rate) from the trend of de-seasoned long-term sea level difference (SLD) between eustatic sea level observed by altimetry and relative sea level observed by tide gauge at coastal stations along the Southern Levantine region.

2. Data and methodology

2.1. Satellite altimetry data

Gridded (1/8° × 1/8°) daily sea level Maps of Absolute Dynamic Topography (MADT) over the Southern Levantine region (30–33.25 °N

Table 1
Comparison of monthly and de-seasoned monthly linear SLR (mm/year) from atmospherically corrected SLA at selected tide gauge stations and co-located altimeter gridded points. And de-seasoned monthly linear sea level difference (altimetry minus tide gauge), which give us the vertical land motion rate (VLM rate) (mm/year), [land subsidence indicated by↓, land uplift indicated by↑ and non-significant land motion indicated by ↔]. Distance between tide gauge and co-located altimeter point (Dist.); correlation of monthly time series (Corr.); root mean square of their difference (RMSD) and completeness index (CI) of the tide gauge time series. Yellow color shows non-significant trend at 95% confidence level.

No	Station Name (country)	longitude	Latitude	Time Span	CI (%)	Tide gauges SLR(mm/year)		Satellite SLR(mm/year)		Comparison			
						Monthly	De-seasoned	Monthly	De-seasoned	VLM rate (mm/year)	Dist. (Km)	Corr.	RMSD (mm)
1	ALEXANDRIA (EGYPT)	29.917	31.217	1993– 2015	96	4.85 ± 1.31	4.65 ± 0.88	4.60 ± 1.16	4.32 ± 0.65	−0.51 ± 0.86 (↔)	3.8	0.80	46
2	Rosetta(EGYPT)	30.368	31.459	2001 – 2015	87	11.18 ± 2.67	11.04 ± 2.25	4.26 ± 1.19	3.98 ± 0.68	−6.21 ± 2.19 (↓)	5.8	0.63	66
3	Burullus (EGYPT)	30.968	31.584	1993– 2015	88	6.08 ± 1.32	5.73 ± 1.32	3.38 ± 1.19	3.09 ± 0.71	−2.73 ± 1.27 (↓)	3.7	0.64	74
4	Damietta(EGYPT)	31.764	31.486	1997 – 2015	95	7. 83 ± 1.99	7.69 ± 1.59	3.69 ± 1.21	3.43 ± 0.69	−4.91 ± 1. 46 (↓)	9.0	0.67	67
5	TEL-AVIV (ISRAEL)	34.767	32.083	1996– 2015	90	1.34 ± 1.37	1.12 ± 0.84	3.73 ± 1.20	3.44 ± 0.67	1.33 ± 0.69 (↑)	7.8	0.86	32
6	HADERA (ISRAEL)	34.863	32.470	1993 – 2012	95	4.82 ± 1.54	4.57 ± 1.00	3.83 ± 1.21	3.53 ± 0.68	−1.85 ± 0.92 (↓)	5.9	0.74	47

and 25 °W–34.5 °E) in the period January 1993–December 2015, were extracted from the satellite multi-mission delayed-time product of the Copernicus Marine Environment Monitoring Service (CMEMS, http://marine.copernicus.eu/) data. This product was produced by merging data from all altimeter missions (Jason-3, Sentinel-3A, HY-2A, Saral/AltiKa, Cryosat-2, Jason-2, Jason-1, T/P, ENVISAT, GFO, ERS1) and spans the period from January 1993 to present. Several corrections have been applied to this data set, including instrumental errors, geophysical effects, tides, and the atmospheric correction using the so-called dynamic atmospheric correction (DAC) was applied too (Carrère and Lyard, 2003; Landerer and Volkov, 2013). The DAC combines the low frequency (time scales greater than 20 days) of the standard inverted barometer (IB) correction with the outputs from MOG2D-G model (Carrère and Lyard, 2003), which improves the representation of high-frequency (time scales less than 20 days) atmospheric forcing as it takes into account both pressure and wind effects (Wöppelmann and Marcos, 2012). The Absolute Dynamic Topography is defined by adding the SLA and the synthetic mean dynamic topography (SMDT), estimated by Rio et al. (2014) over the 1993–2012 period. Data were averaged monthly to use the same temporal resolution as the tide gauge data.

2.2. Tide gauge data

Monthly mean of sea level anomalies data from 6 TG stations (Fig. 1), are used in this study. Four of them are distributed along the Egyptian Mediterranean coast (Alexandria, Rosetta, Burullus and Damietta) and two along the Israel coast (Tel-Aviv and Hadera). The sea level data are based on the hourly record from the Hughes mechanical tide gauges located at Rosetta, Burullus and Damietta are obtained from the Coastal Research Institute in Egypt. Tide gauge record from Alexandria, which proved to show a worthwhile time series (Maiyza and El-Geziry, 2012) and was provided by Prof. El-Geziry (personal communication) updated up to 2009. The record of Alexandria was extended by 6 years of data (2010–2015) that was provided by the University of Hawaii Sea Level Center (UHSLC, http://ilikai.soest.hawaii.edu/uhslc/rqds.html) as hourly, daily and monthly data. Sea level data at the Israel stations were provided by the Permanent Service for Mean Sea Level (PSMSL, http://www.psmsl.org/) as monthly means.

Tel Aviv station has been replaced by Tel Aviv-Yafo (lat. 32.05 °N long 34.75 °E) in October 2010, since the vertical displacement of the reference point is not available, we estimated this datum shift using the altimetry data. Monthly differences of altimeter and tide gauge sea level heights was computed, and each of the two series was modeled, before and after the switchover point (October 2010), with a linear model. The difference between the constant terms of the two models gave an estimation of the vertical datum shift. Also, we apply the same method to correct the datum at the Burullus station due to a change from a floating tide gauge to a radar tide gauge instrument in 2010. While at Alexandria station, jump in datum due to use of two different data source within the same station records, was corrected by assessing the difference in the mean for similar time spans and outliers were removed (Menéndez and Woodworth, 2010). At all tide gauge stations, which used in this study, data sets were quality controlled by analyzing the time series in 1-month segments, data values more than two standard deviations from the mean were removed from the time series and replaced by a linear interpolation for gaps of a few-months duration. Larger gaps were not included in this analysis. See Fig. 2 for the data coverage.

As stated earlier, Altimetry datasets were originally corrected for the dynamic atmospheric correction (DAC). So, the DAC was subtracted from the tide gauge data in order to make it comparable to the altimetry data (Wöppelmann and Marcos, 2012). The dynamic atmospheric correction data with a time resolution of 6 h acquired at the tide gauge stations were extracted with a $0.25^\circ \times 0.25^\circ$ spatial grid resolution from the Auxiliary products dataset, which are freely available at the

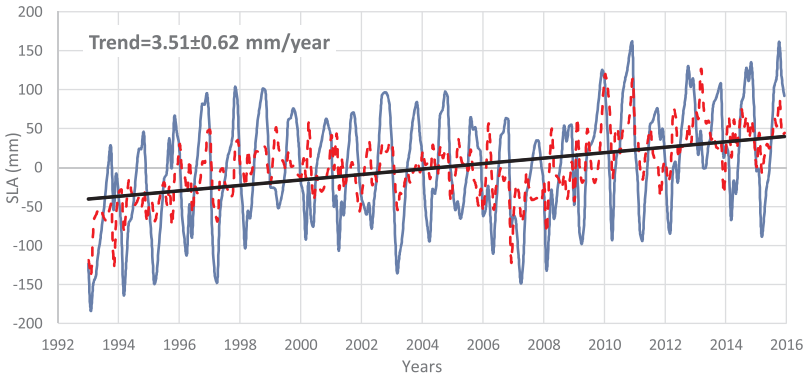

Fig. 4. Monthly averaged time series of SLA (blue line), de-seasonalized (red line) and linear trend (mm/year) (black line) over the Southern Levantine Basin during 1993–2015. (For interpretation of the references to colour in this figure legend, the reader is referred to the web version of this article).

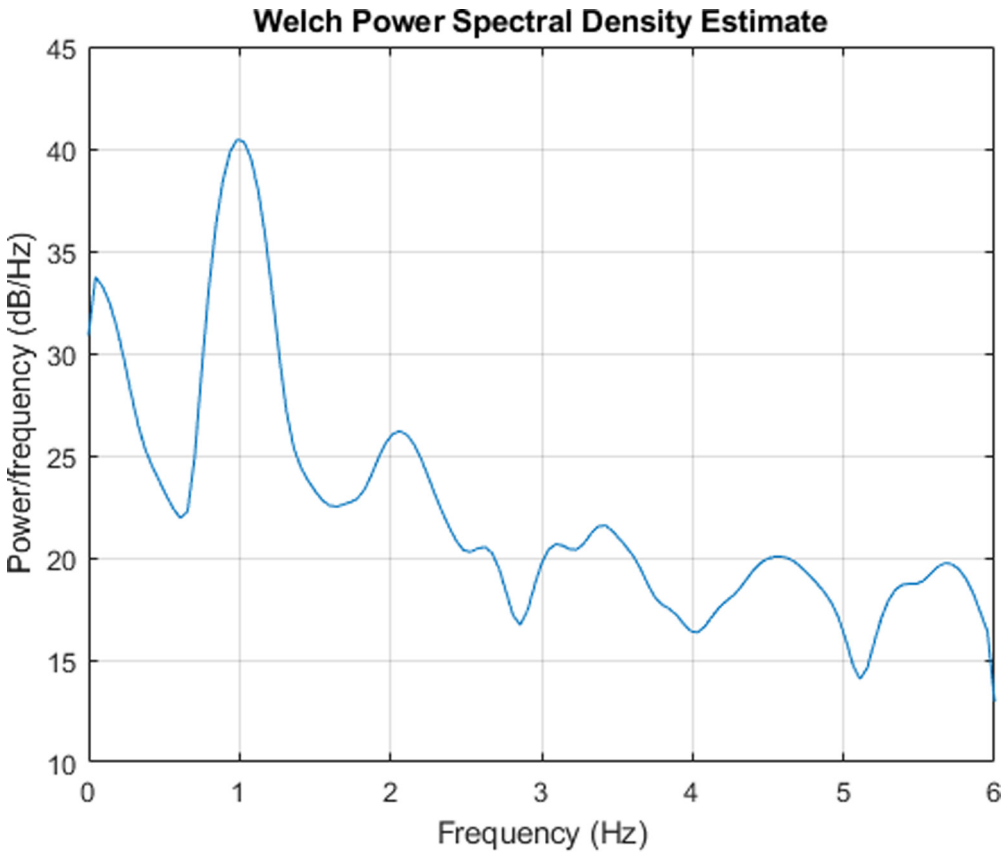

Fig. 5. Welch spectrum of monthly spatial averages of SLA over the Southern Levantine Basin during 1993–2015.

Archiving, Validation, and Interpretation of Satellite Oceanographic (AVISO) website (ftp.aviso.altimetry.fr). Data were averaged monthly in order to use the same temporal resolution as the tide gauge data.

2.3. Estimation of linear trend

For each tide gauge station, an altimeter time series has been selected corresponding to the nearest point in the multi-mission altimeter grid. At each grid point, the mean seasonal cycles were calculated separately for the altimeter and tide gauge time series and then subtracted from the monthly average of each dataset to obtain de-seasoned monthly anomalies. The mean seasonal cycle was estimated by calculating the mean monthly value for each month based on full years only in the interval of analysis, to avoid biases being introduced. The mean value of each month was then removed from all corresponding months in all years to obtain de-seasoned monthly values. At each grid point, the linear trend of the residuals has been estimated separately for the altimeter and tide gauge data with standard least square method (Wilks, 2011).

2.4. Principal component analysis (PCA)

Principal component analysis method (Preisendorfer, 1988) of the residuals (de-seasoned and de-trended time series) was performed to highlight the spatiotemporal sea level variability at inter-annual and decadal time scales. The PCA method is based on a decomposition of a spatiotemporal varying field (here sea level anomaly) into an uncorrelated linear combination of functions of the original variables ranked by variance. The data set is separated into a set of Empirical Orthogonal Function (EOF), which defined the spatial structure, with their associated time series (or the Principal Components PC), which defined the temporal evolution. A significance test was applied based

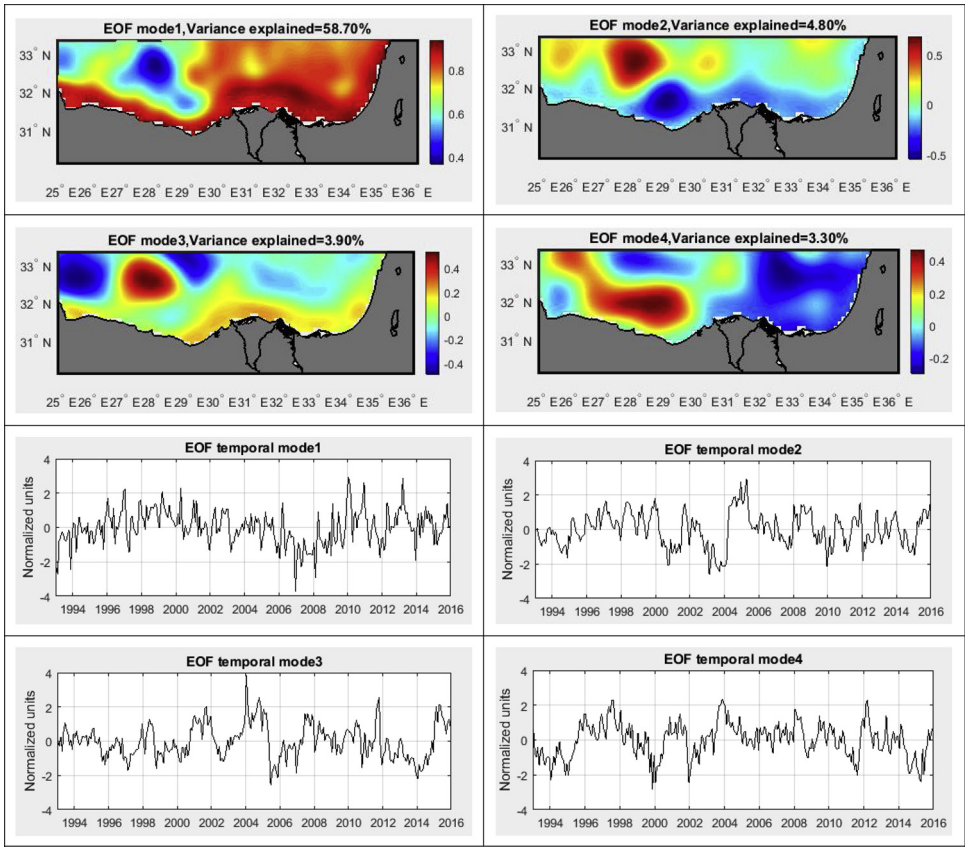

Fig. 6. First four spatial patterns (top) and temporal coefficients (bottom) obtained from the PCA decomposition of the inter-annual and decadal sea level variability in the period 1993–2015.

on a Monte Carlo technique to find the components corresponding to a signal above the noise level (Overland and Preisendorfer, 1982). The input data to the PCA were first de-trended and normalized to standardized anomalies by dividing each point time-series by its standard deviation, to avoid that a point with high variability dominates the analysis, and the output spatial vectors are normalized to the maximum value for each mode according to Fenoglio-Marc (2002).

2.5. Estimation of vertical land motions

Sea level measured by altimetry is relative to the geocenter and is therefore independent from vertical land motion (i.e. Absolute Sea Level, ASL), while the sea level measured by a tide gauge station is relative to the Earth's crust and is therefore affected by vertical land motion (i.e. Relative Sea Level, RSL). For this reason, the vertical land motion is contained in the long-term component of sea level difference (SLD) between satellite altimetry and tide gauge (Nerem and Mitchum, 2002; Fenoglio-Marc et al., 2004, 2012). Vertical land motion (VLM rate) were estimated, for a set of 6 TG sites, from the trend of de-seasoned monthly averages of SLD.

3. Results and discussion

3.1. Absolute sea level (ASL) linear trend mapping from altimetry data

Fig. 3 presents the absolute sea level trend map over the Southern Levantine basin for the period 1993–2015. The results clearly showed that the absolute sea level trends were positive throughout the Southern Levantine region and ranged from 0.5 to 5.5 mm/year. The highest trends were found in the Mersa-Matruh gyre (up to 5.5 mm/year, in agreement with Shaltout et al., 2015) and in Shikmona gyre (up to 4.5 mm/year). Trends were generally lower than 4 mm/year in the Eastern Nile Delta and Israel coasts, while in the Western Nile Delta the trends were more than that value. Trends taken between 1993 and 2015 gave 3.1–4.3 mm/year at the co-located altimeter time series in Alexandria, Rosetta, Burullus, Damietta, Tel-Aviv and Hadera (Table 1, column 10).

Fig. 4 shows the spatial mean of level anomaly (SLA) time-series during the period from 1993 to 2015, which clearly indicated strong seasonal signals (annual and semi-annual), as well as inter-annual variability. The de-seasonal variation, after the seasonality has been removed through calculating the monthly climatological means showed that the mean rate (Linear trend) of SLR is 3.51 ± 0.62 mm/year. The spatial averaged of SLA time-series, were spectrally analyzed using the Welch method (Welch, 1967) in the Southern Levantine region (Fig. 5). The first dominant component corresponds to the annual signals are dominant with amplitude of 10.4 cm, while the second dominant component corresponds to decadal fluctuations (124 months ≈10 years) with amplitude of 4.7 cm.

The principal component analysis (PCA) is applied to the residuals of SLA time series after standardization, i.e. each time-series is de-meaned and divided by the standard deviation to avoid that a point with high variability that might dominate the analysis. The first four modes were statistically significant and explained together 70.7% of the variance of sea level during 1993–2015. The first EOF mode, which accounted for approximately 58.7% of the total variance, showed that every point has the same sign (here taken as positive), implying an oscillation of the entire region moving up or down in phase (see Fig. 6, top). From the corresponding PC time series (Fig. 6, bottom), the highest positive peak of the inter-annual variability was encountered in winter of 2010, which was occurred throughout a strong negative phase of the North Atlantic Oscillation (Landerer and Volkov, 2013). While the highest negative peak was observed in winter of 2007.

The second EOF mode, which explained about 4.8% of the total

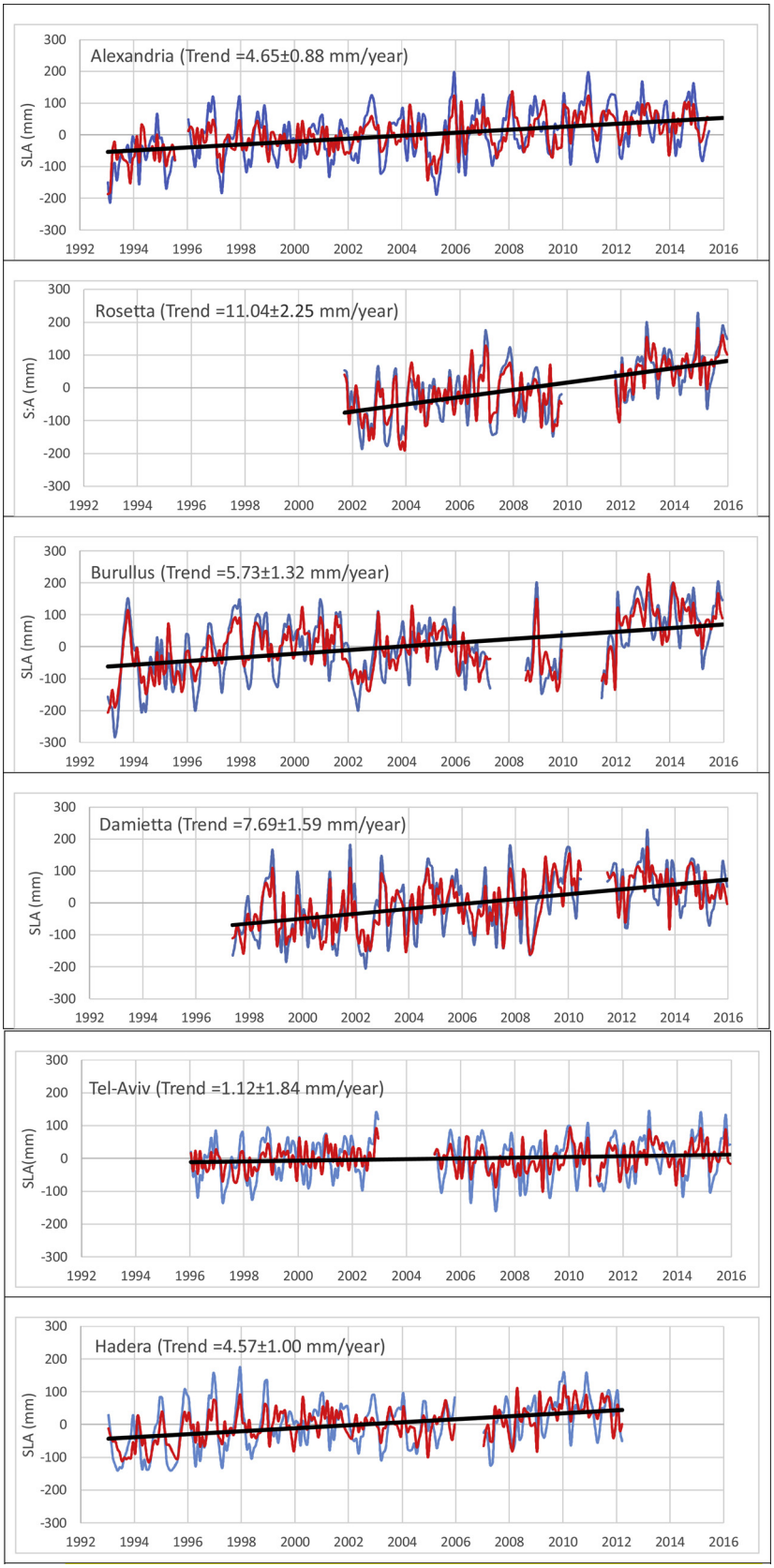

Fig. 7. The atmospherically corrected SLA of monthly (blue), de-seasoned monthly (red) time series and linear de-seasoned trends (mm/year) (black) for the available TG stations in the Southern Levantine Basin. (For interpretation of the references to colour in this figure legend, the reader is referred to the web version of this article).

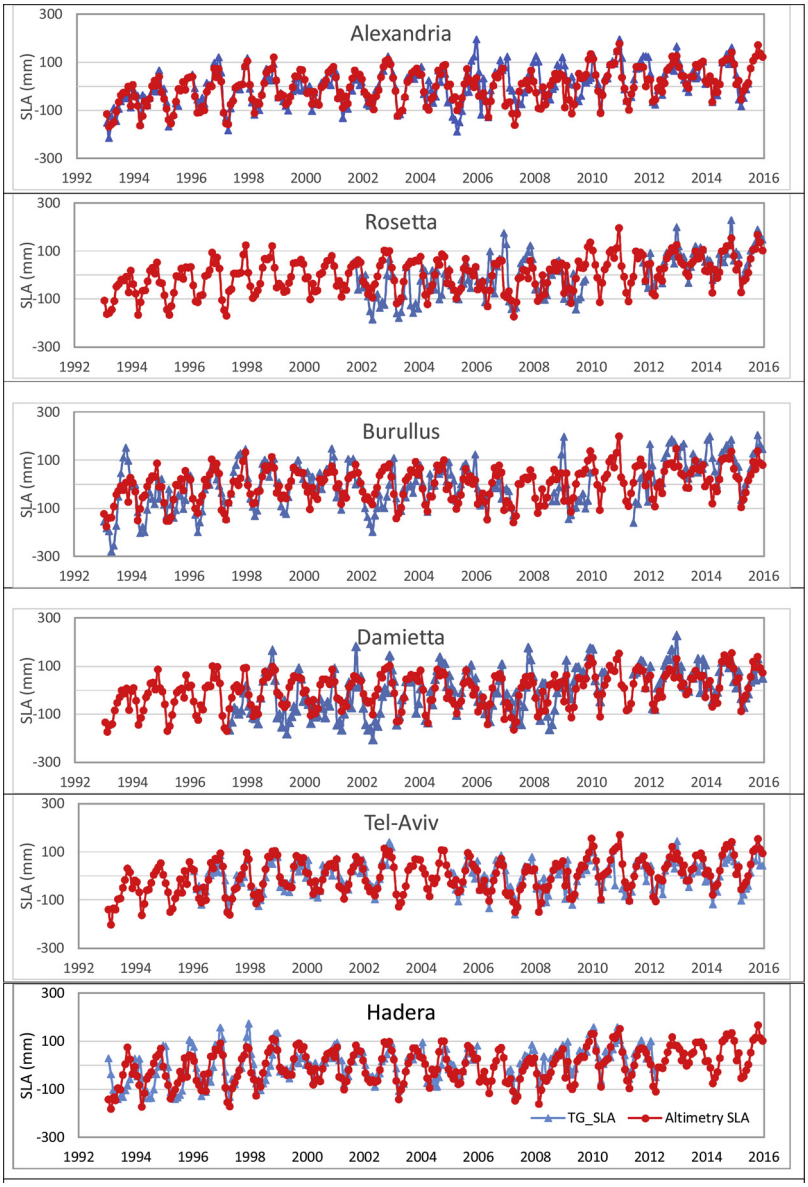

Fig. 8. Comparison between Sea level anomaly (SLA) derived from satellites altimetry (circle) and tide gauge data (triangle).

variance was corresponding to sea level variability out of phase in the Mersa-Matruh gyre and rest of the region, meaning an SLA rise in the former and drop in the latter. The third and fourth modes (3.9% and 3.3% of the total variance) represented a sub-regional variability in the Southern Levantine region.

3.2. Relative sea level (RSL) linear trend from TG data

Sea level anomalies data at the six selected TG stations (Alexandria, Rosetta, Burullus, Damietta, Tel-Aviv and Hadera) have been corrected for the DAC effect. The atmospherically corrected linear trends of monthly and de-seasoned monthly means of SLA data were estimated and summarized in (Table1; columns 7&8). Five stations showed significant and positive trends at 95% confidence interval, while only one station in Israel (Tel-Aviv) had insignificant monthly trend (1.34 ± 1.37 mm/year). The uncertainty of the monthly linear trends was higher than that for de-seasoned one.

Fig. 7 demonstrates the monthly and de-seasoned monthly averaged time series of atmospherically corrected SLA, and linear de-seasoned trends for different TG stations of the Southern Levantine region during the period of study (as shown in Table 1; column 5). Significant spatial variability of the relative sea level linear trends was found, and ranged from 1.12 ± 0.84 mm/year at Tel-Aviv station in Israel to 11.04 ± 2.25 mm/year at Rosetta station in Egypt.

3.3. Vertical land motion

In this section, the sea level anomaly data from satellite altimeter was compared with ground truth (tide gauge) data (Fig. 8). The results of the sea level comparison are focused on the pattern and the correlation analysis between altimetry and tide gauge sea level anomaly (SLA) data. The comparison of sea level from altimetry and tide gauge data has been done by extracting the monthly mean of SLA at the tide gauge locations and the altimeter grid point that were nearby the tide gauge stations. The correlations and root mean square differences (RMSD) of the regression between the tide gauge and the nearest satellite altimeter grid point time series were chosen to measure the goodness of the fit. The smaller the RMSD the larger similarity between high and low values of satellite altimeter and tide gauges.

Table 1 summarizes the results. The best agreement between

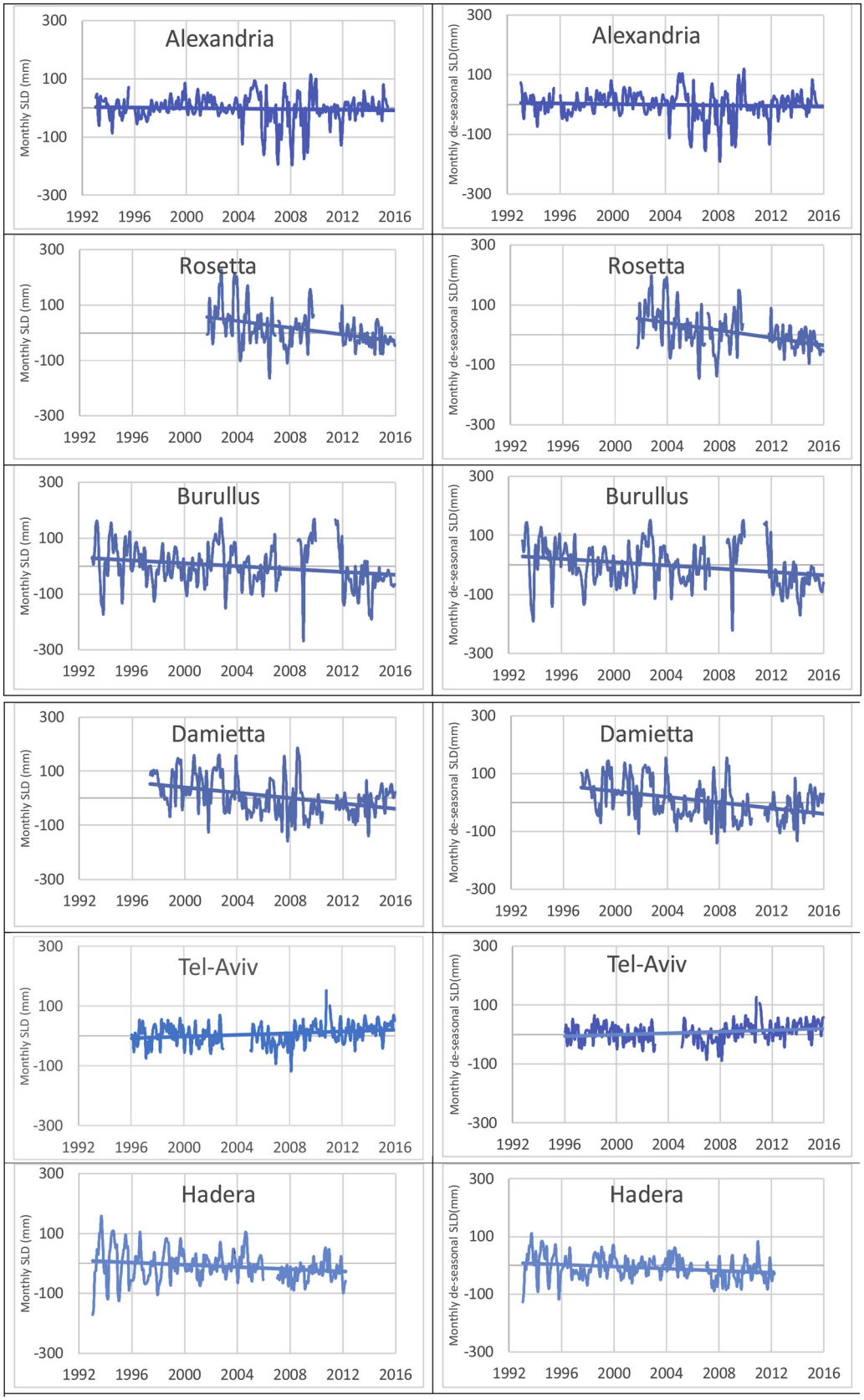

Fig. 9. Anomalies of sea level differences (Altimetry-TG) at the stations of Alexandria, Rosetta, Burullus, Damietta, Tel-Aviv and Hadera, corresponding to monthly averages (left), and de-seasoned monthly averages (right).

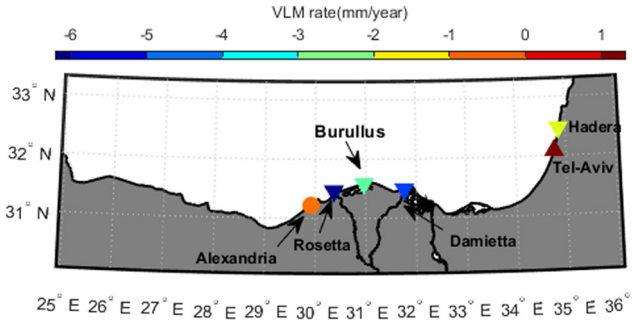

Fig. 10. Vertical land motion estimated from de-seasoned monthly differences of sea level Anomalies from altimetry and tide gauge data. Triangles pointing up and down represent land uplift and subsidence, respectively. Circle indicate insignificant land motion at Alexandria station.

altimetry and tide gauge sea level time-series was found at Tel-Aviv (correlation 0.86, RMSD 32 mm for monthly time series) and at Alexandria (correlation 0.80 and RMSD 46 mm), whereas the lowest agreement occurred in Rosetta (correlation 0.63 and RMSD 66 mm). In general, satellite altimetry and tide gauge signals were comparable in most of the cases considered.

Fig. 9 shows the SLD obtained using monthly and de-seasoned monthly data at the six stations of Alexandria, Rosetta, Burullus, Damietta, Tel-Aviv and Hadera. The standard deviation of the differences is higher for monthly values, part of the differences was due to the differential variability at the station and at the altimeter point. The trend of the de-seasonalized "altimetric minus tide gauge" time series (called "VLM rate") were shown in Table1 (column 11) and in Fig. 10. Positive linear trends represented land uplift, while negative ones represented land subsidence. So, Fig. 10 presents positive trends using triangles pointing up and negative ones by triangles pointing down. Circle in the figure represented insignificant land motion at Alexandria station.

In Egypt, at Alexandria station, insignificant land motion was detected with VLM rate of -0.51 ± 0.86 mm/year). Accordingly, the Alexandria coastal plain is moderately stable, with estimates of 0 to -0.5 mm/year land subsidence (Frihy et al., 2010). At the other three stations which distributed along the Nile Delta, a significant subsidence at the 95% level, was detected. In Rosetta, the VLM rate was (−6.21 ± 2.19 mm/year). In Burullus, the VLM rate was (−2.73 ± 1.27 mm/year). Subsidence was also found in Damietta (−4.91 ± 1.46 mm/year). In the two Nile river mouth stations (Damietta and Rosetta), the trend of the tide-gauge derived sea level was two and three times larger than the altimetric sea level trend.

In Israel, at Tel-Aviv station, tide gauge time series have low trend (1.12 ± 0.84 mm/year), and a small land uplift was detected with VLM rate of (1.33 ± 0.69 mm/year). At the other station (Hadera), a significant subsidence at the 95% level, was detected. The VLM rate was (−1.85 ± 0.92 mm/year), it was in good agreement with the vertical land movement result of García et al. (2007) inferred from altimetry and tide gauge differences (−2.4 ± 1.5 mm/year).

4. Conclusions

The main goal of this work was to provide an estimation of the vertical land motion (VLM rate) along the Southern Levantine coastline from altimetry and TG sea level data. The average rates of absolute eustatic sea level rise derived from satellite altimetry through 23-year long (1993–2015) was 3.51 ± 0.62 mm/year. This is slightly higher than the global mean rate of 3.19 ± 0.63 mm/year during the same period from altimetric data (Chambers et al., 2017). Sea level trends taken between 1993 and 2015 were 3.1–4.3 mm/year near selected tide gauge stations. Also, all the tide gauge stations showed a positive trend, the relative sea-level rise ranged from 1.12 ± 0.84 mm/year at Tel-Aviv station in Israel to 11.04 ± 2.25 mm/year at Rosetta station in Egypt. The average eustatic sea level rise represented around from 35% to 60% of total relative sea-level rise measured along Nile Delta region.

The vertical land movement (VLM rate) have been resolved at an arrangement of 6 TG stations by differencing the tide gage sea level time-series with a comparable time-series got from closest Satellite altimetry grid point and by figuring the linear trend of the differences. This technique, represented an interesting alternative to the use of collocated GPS at the tide gauge stations when GPS is not available. A significant land subsidence at the 95% level was detected the in-Nile Delta region (VLM rates were −6.21 ± 2.19, −2.73 ± 1.27 and −4.91 ± 1.46 mm/year in Rosetta, Burullus and Damietta, respectively), which are in good agreement with Stanley and Clemente (2017). While at Alexandria station, insignificant land motion was detected with VLM rate of −0.51 ± 0.86 mm/year. This was in a good agreement with (Frihy et al., 2010). Also, land uplift was detected at Tel-Aviv station in Israel with VLM rate (1.33 ± 0.69 mm/year), while at Hadera station land subsidence was detected with VLM rate (−1.85 ± 0.92 mm/year) in agreement with García et al. (2007).

In conclusion, Nile Delta climate-related sea level trend was found to be reinforced by vertical land movements of a similar or even larger magnitude and that its impact on coastal areas should be seriously considered. The determination of vertical land movements constitutes therefore a key step towards identifying the different forcing factors contributing to sea level change at the coastal area. This may help in correctly quantifying their relative importance, enhancing our understanding of the causes for robust predictions and full assessment of coastal vulnerability by sea level rise. So, our recommendations for all policy and decision makers are to increase the number and geographical distribution of the tide gauges in conjunctions with continuous GPS. Further analysis with new data types and longer time series are also recommended.

Acknowledgments

We would like to acknowledge all organizations that provided the source data used in this analysis, including coastal research institute in Egypt for providing tide gauge data, CMEMS Project for the altimetry products, and AVISO Project for Dynamic Atmospheric Correction (DAC) data, the permanent Service for Mean Sea Level (PSMSL), and University of Hawaii Sea Level Center (UHSLC). We wish to thank the contribution of Prof. El-Geziry for the preparation of part of the tide gauge data at Alexandria station. We would like also to thank Prof. Saad Mesbah for his constructive remarks. Special thanks to the associate editor Dr. Volker Klemann and the two anonymous reviewers for their constructive and helpful comments on the manuscript.

References

Bonaduce, A., Pinardi, N., Oddo, P., Spada, G., Larnicol, G., 2016. Sea-level variability in the Mediterranean Sea from altimetry and tide gauges. Clim. Dyn. 47 (9-10), 2851–2866.

Carrère, L., Lyard, F., 2003. Modeling the barotropic response of the global ocean to atmospheric wind and pressure forcing-comparisons with observations. Geophys. Res. Lett. 30 (6).

Chambers, D.P., Cazenave, A., Champollion, N., Dieng, H., Llovel, W., Forsberg, R., et al., 2017. Evaluation of the global mean sea level budget between 1993 and 2014. Surv. Geophys. 38 (1), 309–327.

Dasgupta, S., Laplante, B., Meisner, C., Wheeler, D., Yan, J., 2009. The impact of sea level rise on developing countries: a comparative analysis. Clim. Change 93 (3), 379–388.

El-Din, K.A., Abdelrahman, S.M., El Meligy, M., 2007. Seasonal and long term variations of sea level and meteorological conditions along the Egyptian coasts. In: MEDCOAST. Proceedings of the Eighth International Conference on the Mediterranean Coastal Environment Vol. 7. pp. 1295–1307.

Ericson, J.P., Vörösmarty, C.J., Dingman, S.L., Ward, L.G., Meybeck, M., 2006. Effective sea-level rise and deltas: causes of change and human dimension implications. Glob. Planet. Change 50 (1), 63–82.

Fenoglio-Marc, L., 2002. Long-term sea level change in the Mediterranean Sea from multi-satellite altimetry and tide gauges. Phys. Chem. Earth Parts A/b/c 27 (32-34), 1419–1431.

Fenoglio-Marc, L., Dietz, C., Groten, E., 2004. Vertical land motion in the Mediterranean

Sea from altimetry and tide gauge stations. Mar. Geod. 27 (3-4), 683–701.
Fenoglio-Marc, L., Schöne, T., Illigner, J., Becker, M., Manurung, P., Khafid, 2012. Sea level change and vertical motion from satellite altimetry, tide gauges and GPS in the indonesian region. Mar. Geod. 35 (SUPPL. 1), 137–150. https://doi.org/10.1080/01490419.2012.718682.
Frihy, O.E.S., Deabes, E.A., Shereet, S.M., Abdalla, F.A., 2010. Alexandria-Nile Delta coast, Egypt: update and future projection of relative sea-level rise. Environ. Earth Sci. 61 (2), 253–273.
García, D., Vigo, I., Chao, B.F., Martínez, M.C., 2007. Vertical crustal motion along the mediterranean and black sea coast derived from ocean altimetry and tide gauge data. Pure Appl. Geophys. 164 (4), 851–863. https://doi.org/10.1007/s00024-007-0193-8.
García, F., Vigo, M.I., García-García, D., Sánchez-Reales, J.M., 2011. Combination of multisatellite altimetry and tide gauge data for determining vertical crustal movements along Northern Mediterranean Coast. Pure Appl. Geophys. 169 (8), 1411–1423.
Haddad, M., Hassani, H., Taibi, H., 2013. Sea level in the Mediterranean Sea: seasonal adjustment and trend extraction within the framework of SSA. Earth Sci. Inform. 6 (2), 99–111. https://doi.org/10.1007/s12145-013-0114-6.
Hassaan, M.A., Abdrabo, M.A., 2013. Vulnerability of the Nile Delta coastal areas to inundation by sea level rise. Environ. Monit. Assess. 185 (8), 6607–6616.
Landerer, F.W., Volkov, D.L., 2013. The anatomy of recent large sea level fluctuations in the Mediterranean Sea. Geophys. Res. Lett. 40 (3), 553–557.
Maiyza, I.A., El-Geziry, T.M., 2012. Long term sea-level variation in the south-eastern Mediterranean Sea: a new approach of examination. J. Oper. Oceanogr. 5 (2), 53–59.
Menéndez, M., Woodworth, P.L., 2010. Changes in extreme high water levels based on a quasi-global tide-gauge data set. J. Geophys. Res. Oceans 115 (C10).
Nagy, H., Elgindy, A., Pinardi, N., Zavatarelli, M., Oddo, P., 2017. A nested pre-operational model for the egyptian shelf zone: model configuration and validation/calibration. Dyn. Atmos. Ocean. 80, 75–96. https://doi.org/10.1016/j.dynatmoce.2017.10.003.
Nerem, R.S., Mitchum, G.T., 2002. Estimates of vertical crustal motion derived from differences of TOPEX/POSEIDON and tide gauge sea level measurements. Geophys. Res. Lett. 29 (19).
Nicholls, R.J., Cazenave, A., 2010. Sea-level rise and its impact on coastal zones (science (1517)). Science 329 (5992), 628.
Overland, J.E., Preisendorfer, R.W., 1982. A significance test for principal components applied to a cyclone climatology. Mon. Weather. Rev. 110 (1), 1–4.
Preisendorfer, R.W., 1988. Principal Component Analysis in Meteorology and Oceanography, no. 17 in Developments in Atmospheric Science. Elsevier, Amsterdam.
Raey, M., 2010. In: Michel, D., Pandya, A. (Eds.), Coastal Zones and Climate Change. Stimson Center, pp. 31–50. Rep. Retrieved from. http://www.jstor.org/stable/resrep10902.9.
Rio, M.H., Pascual, A., Poulain, P.M., Menna, M., Barceló, B., Tintoré, J., 2014. Computation of a new mean dynamic topography for the Mediterranean Sea from model outputs, altimeter measurements and oceanographic in situ data. Ocean. Sci. 10 (4), 73.
Shaltout, M., Tonbol, K., Omstedt, A., 2015. Sea-level change and projected future flooding along the Egyptian Mediterranean coast. Oceanologia 57 (4), 293–307.
Solomon, S., Qin, D., Manning, M., Chen, Z., Marquis, M., Averyt, K.B., et al., 2007. The Physical Science Basis. Contribution of Working Group I to the Fourth Assessment Report of the Intergovernmental Panel on Climate Change. Cambridge University Press, Cambridge, pp. 996.
Stanley, J.-, Clemente, P.L., 2017. Increased land subsidence and sea-level rise are submerging egypt's nile delta coastal margin. GSA Today 27 (5), 4–11. https://doi.org/10.1130/GSATG312A.1.
Stanley, J.D., Toscano, M.A., 2009. Ancient archaeological sites buried and submerged along Egypt's Nile delta coast: gauges of Holocene delta margin subsidence. J. Coast. Res. 158–170.
Tsimplis, M.N., Calafat, F.M., Marcos, M., Jordà, G., Gomis, D., Fenoglio-Marc, L., et al., 2013. The effect of the NAO on sea level and on mass changes in the Mediterranean Sea. J. Geophys. Res. Oceans 118 (2), 944–952. https://doi.org/10.1002/jgrc.20078.
Welch, P., 1967. The use of fast Fourier transform for the estimation of power spectra: a method based on time averaging over short, modified periodograms. Ieee Trans. Audio Electroacoust. 15 (2), 70–73.
Wilks, D.S., 2011. Statistical Methods in the Atmospheric Sciences Vol. 100 International Geophysics Series https://doi.org/0127519661.
Wöppelmann, G., Marcos, M., 2012. Coastal sea level rise in southern Europe and the nonclimate contribution of vertical land motion. J. Geophys. Res. Oceans 117 (C1).
Wöppelmann, G., Le Cozannet, G., Michele, M., Raucoules, D., Cazenave, A., Garcin, M., et al., 2013. Is land subsidence increasing the exposure to sea level rise in Alexandria, Egypt? Geophys. Res. Lett. 40 (12), 2953–2957.